

The X-ray variability of high redshift QSOs

J. Manners, O. Almaini, A. Lawrence

Institute for Astronomy, University of Edinburgh, Royal Observatory, Blackford Hill, Edinburgh EH9 3HJ

MNRAS accepted 22 October 2001

ABSTRACT

We present an analysis of X-ray variability in a sample of 156 radio quiet quasars taken from the ROSAT archive, covering a redshift range $0.1 < z < 4.1$. A maximum likelihood method is used to constrain the amplitude of variability in these low signal to noise light curves. Through combining these data in ensembles we are able to identify trends in variability amplitude with luminosity and with redshift. The decline in variability amplitude with luminosity identified in local AGN ($z < 0.1$) is confirmed out to $z = 2$. There is tentative evidence for an increase in QSO X-ray variability amplitude towards high redshifts ($z > 2$) in the sense that QSOs of the same X-ray luminosity are more variable at $z > 2$. We discuss possible explanations for this effect. The simplest explanation may be that high redshift QSOs are accreting at a larger fraction of the Eddington limit than local AGN.

Key words: galaxies: active – galaxies: evolution – galaxies: nuclei – quasars: general – X-rays: general – X-rays: galaxies

1 INTRODUCTION

Rapid X-ray variability appears to be very common in AGN (e.g. Turner 1988). Light curves can often look qualitatively very different, but they generally appear completely random in nature with no characteristic time-scales or periodicities, indicating there are no long-lived orbiting components. Power spectra show ‘red noise’ (i.e. more power at lower frequencies), with the form $P(f) \propto f^{-\alpha}$ where $\alpha \approx 1.5$ (Lawrence & Papadakis 1993, Green et al 1993). Departures from a featureless power spectrum are rare. Some evidence for quasi-periodic oscillations has been observed in NGC 5548, NGC 4051 (Papadakis & Lawrence 1993, 1995) and IRAS 18325-5926 (Iwasawa et al 1998), and in a handful of AGN a turnover has been seen at low frequencies (e.g. Edelson & Nandra 1999). A high frequency cut-off would indicate the size of the emission region, although this cannot yet be distinguished from the noise for even the most well studied AGN. Simulated light curves based on the existence of a number of independent flaring regions (i.e. exponential shots) can reproduce the shape of the power spectrum only when the shots are allowed to vary in time-scale. Beyond this, models are difficult to constrain (Green et al 1993).

Variability studies of local AGN ($z < 0.1$) indicate that more luminous sources vary with a lower amplitude. This may be explained if more luminous sources are physically larger in size, so that they are actually varying more slowly. Alternatively, they may contain more independently flaring regions and so have a genuinely lower amplitude. The slope of this correlation has been calculated in a number of papers using overlapping samples of local AGN. Lawrence & Papadakis (1993) and Green et al (1993) analyzed samples of light curves from the EXOSAT database. The variability amplitude was found to vary with luminosity as $\sigma \propto L_X^{-\beta}$ with $\beta \approx 0.3$. The most comprehensive analysis of the variability-

luminosity relation was carried out by Nandra et al, 1997 (hereafter N97) for 18 local Seyferts observed with the ASCA satellite. They find $\beta = 0.355 \pm 0.015$. Whether this well-defined correlation applies to high redshift QSOs is not so clear. Observations of distant QSOs are generally of low signal-to-noise and measurements of variability in individual objects are poorly defined. Almaini et al (2000) developed a technique to measure the amplitude of variability for low signal-to-noise sources and thus high-redshift AGN. By combining light curves from a number of AGN they were able to measure the amplitude of variability over ranges in luminosity and redshift. They studied a sample of 86 QSOs from the Deep ROSAT Survey of Shanks et al (1991) spanning a wide range in redshift ($0.1 < z < 3.2$). The behaviour of variability amplitude with luminosity was found to be in rough agreement with the anti-correlation seen in local AGN but showing a possible upturn for the most luminous sources. Tentative evidence suggested this was due to increased variability at high redshifts, although a definite trend in the redshift behaviour could not be clearly confirmed.

In this paper we use the techniques of Almaini et al (2000) to determine the amplitude of variability in an expanded sample of QSOs taken from the ROSAT archive. QSOs at $z > 1$ are preferentially selected in order to constrain the redshift behaviour of X-ray variability. A cosmology with $q_0 = 0.5$, $H_0 = 50 \text{ km s}^{-1} \text{ Mpc}^{-1}$ is used throughout.

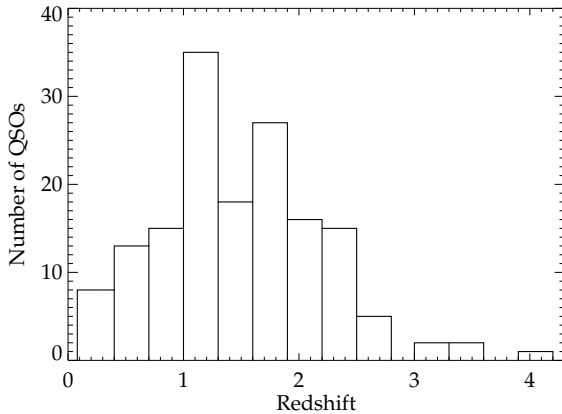
2 THE SAMPLE

The sample consists of 156 QSOs between $0.08 < z < 4.11$ taken from the ROSAT PSPC archive. It is made up of QSOs taken from a number of sources that all adhere to the following selection criteria:

arXiv:astro-ph/0110461v1 22 Oct 2001

Table 1. Samples selected from the ROSAT PSPC archive.

Subsample	Notes	No. QSOs
Deep ROSAT Survey (Shanks et al. 1991)	7 deep ROSAT pointings with exposures from 30 - 80ks over 2-14 days. Broad emission line QSOs, FWHM > 1000 km s ⁻¹ (Detailed in Almaini et al. 2000.)	84
ROSAT Radio Quiet Quasar catalogue (LEDAS)	Cross-correlation of ROSAT archive sources with the Veron 1993 catalogue for radio quiet 'broad emission line' objects with z > 1	28
ROSAT deep survey of the Lockman Hole (Hasinger et al. 1998)	Data taken from single 65ks exposure, to measure short time-scale variations. Object classes a - c selected (broad line AGN). IDs taken from Schmidt et al. 1998.	14
Deep ROSAT Survey (McHardy et al. 1998)	Data taken from the longer first exposure of 73ks. Broad emission line objects selected (FWHM > 1000 km s ⁻¹)	13
Veron 2000 cross-correlated with ROSAT archive sources (LEDAS)	Acts as an update to the ROSAT RQQ catalogue. QSOs selected with z > 2, undetected in radio. Veron QSOs are defined to have 'broad emission lines'.	17
Total:		156

Figure 1. Redshift distribution of our sample of 156 radio quiet quasars.

- ID: radio quiet quasar
- X-ray exposure > 10,000 seconds
- Flux signal-to-noise > 5
- Within 20 arcmin of ROSAT pointing
- Optimal re-binning (see section 3) gives at least 3 time bins

The sample can be broken down into 5 subsamples, individually selected to cover the luminosity and redshift parameter space. These are listed in Table 1. Only PSPC data was used for reasons of consistency and ease of data reduction. The redshift distribution of the entire sample is displayed in Fig. 1.

3 DATA REDUCTION

The data were obtained from the LEDAS online database facility at Leicester. Data reduction was performed with the Asterix X-ray data processing package. Each source was extracted using a circular mask of radius chosen to include 90 per cent of the PSF. The data was then filtered to remove periods of high particle background characterized by the Master Veto Rate rising above 170 counts s⁻¹. Additional filtering restricted the energy range to 0.1 – 2.4 keV.

Careful background subtraction was extremely important to ensure measurement of source variability was not compromised. Background regions were chosen to be as close as possible to the

source to minimize the effects of any background gradients. Areas of at least 5 arcmin radius were used. These were large enough to smear out background irregularities due to undetected sources. A number of further regions were selected and compared with the first to ensure that our chosen region did not contain any abnormalities. Finally, the background light curve was compared with the source light curve and a linear correlation coefficient computed. If a highly significant correlation (or anti-correlation) was found the data was reduced again using a different background region.

Binning of the light curves was initially constrained by the orbit of the satellite. ROSAT's low altitude (580km), and overheads led to a typical exposure of 1000-2000 seconds per 96 minute orbit. The light curves were therefore binned on these periodic orbits. An algorithm was then used to bin up the data to allow meaningful Gaussian statistics. Re-binning of light curves can be approached in a number of ways, and important data may be lost if the method used is over-simplified. The algorithm constructed uses the mean intensity of the source to identify bins that would nominally contain less than 15 photons. These bins are merged with the neighbouring bin that has been merged the least number of times. Where large gaps in the data are identified (> 5 hours), bins will be discarded rather than merged with data many orbits away. Light curves with less than 3 time bins were not used for the variability analysis.

In order to remain consistent, all measurements of X-ray luminosity are made through extraction of fluxes from the same datasets used for the variability analysis.

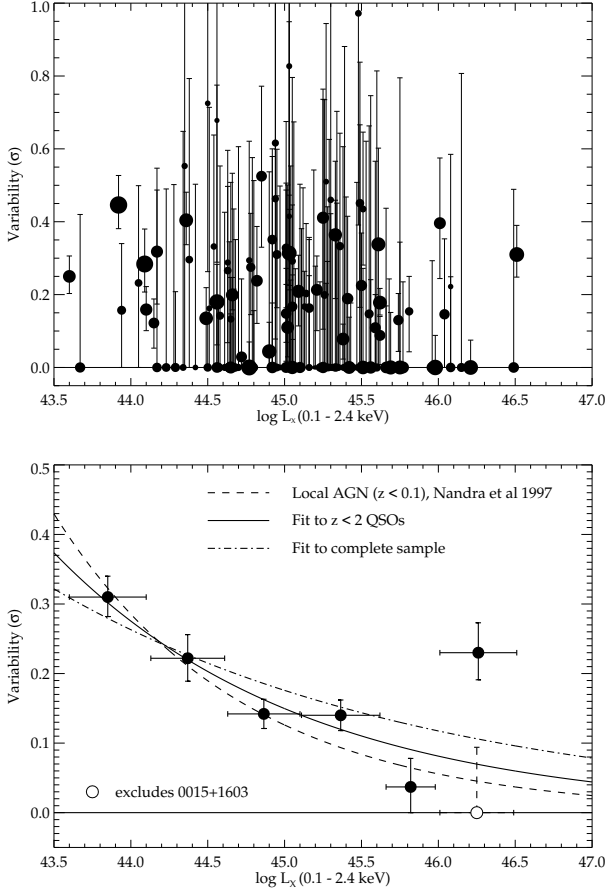
4 MEASURING VARIABILITY

The method used for measuring the amplitude of intrinsic variability is fully described in Almaini et al (2000). To compare objects of different flux, the light curves are divided by the mean, so that measurements of *fractional* variability are made. A maximum likelihood technique is used to separate the intrinsic variations in the light curve from those due to noise. The likelihood for values of QSO variability amplitude (σ_Q) is given by:

$$L(\sigma_Q | x_i, \sigma_i) = \prod_{i=1}^N \frac{\exp \left\{ -\frac{1}{2} (x_i - \bar{x})^2 / (\sigma_i^2 + \sigma_Q^2) \right\}}{(2\pi)^{1/2} (\sigma_i^2 + \sigma_Q^2)^{1/2}} \quad (1)$$

where x_i are data points with mean \bar{x} (1 in this case) and σ_i are the measurement errors. The maximum likelihood estimate for σ_Q is obtained from the peak of the distribution. The errors are measured

Figure 2. (a) Maximum likelihood estimates for the variability amplitude as a function of luminosity for the 156 QSOs. The size of the points indicate relative flux. In (b) we display the results in ensemble form (the vertical scale has been changed). Note, these are calculated from the original light curves and are not averages of the individual likelihood estimates (see section 4). The exclusion of QSO 0015+1603 is explained in section 6.

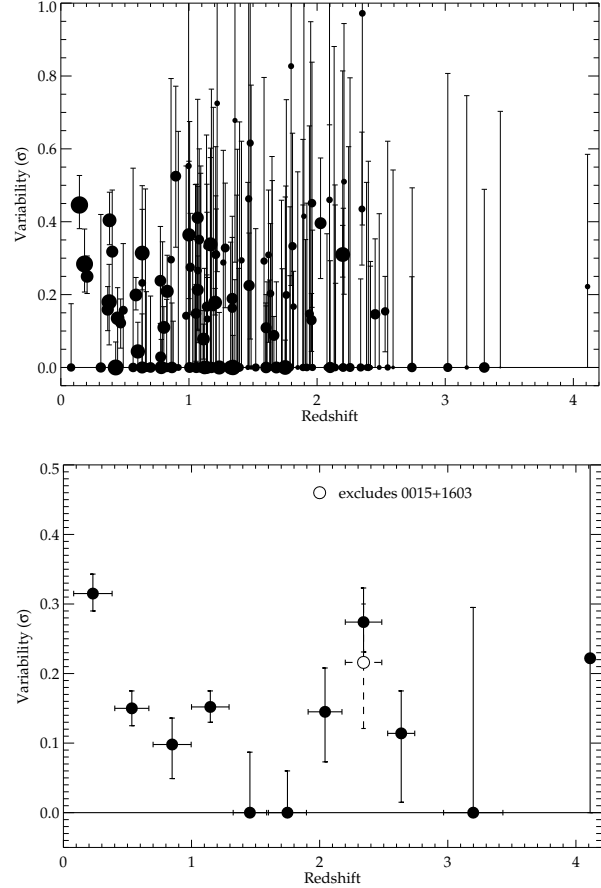


by finding limits of equal likelihood that enclose 68 per cent of the area under the likelihood curve.

The majority of the light curves analyzed here are of low signal-to-noise which in many cases can only give us an upper limit on the amplitude of variability. In order to extract meaningful information from the sample it was necessary to combine the light curves into ensembles over given ranges of luminosity or redshift. To do this we assume that all the quasars in an ensemble have the same intrinsic variability. We can then exploit the fact that variance does not depend on the order of the measurements to effectively combine all the light curves into one ‘ensemble light curve’. The amplitude of intrinsic variability can then be measured as for a single object. This provides a more comprehensive, accurate and unbiased method of determining variability within an ensemble than simply taking an average of the individual maximum likelihood estimates. Of course, if the quasars in a given luminosity or redshift bin actually have a range of intrinsic variabilities, our estimate may be biased towards the most variable members. We discuss this possibility in section 6.

A number of corrections must be made to the variability measurements before they can be compared in an unbiased way. The serendipitous nature of this sample means that light curve observations have a range of total integration times and sampling rates.

Figure 3. (a) Maximum likelihood estimates for the variability amplitude as a function of redshift for the 156 QSOs. The size of the points indicate relative flux. In (b) we display the results in ensemble form (the vertical scale has been changed). Note, these are calculated from the original light curves and are not averages of the individual likelihood estimates (see section 4). The exclusion of QSO 0015+1603 is explained in section 6.



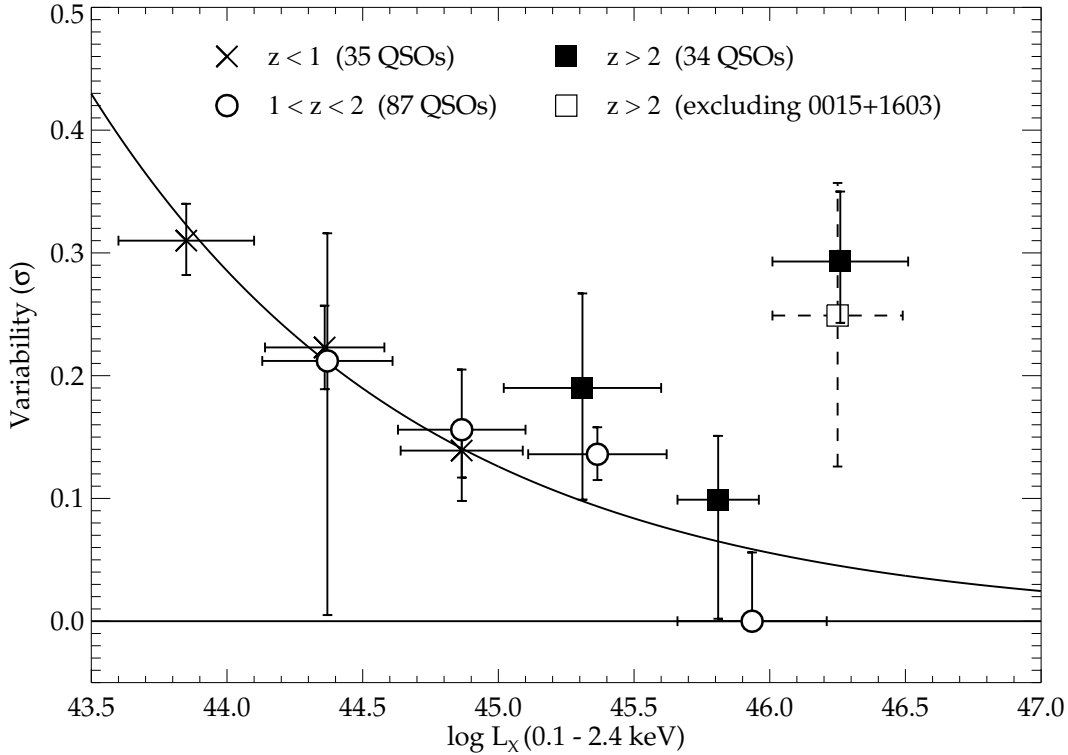
QSO power spectra show ‘red noise’ indicating that the observed amplitude of variability will increase with length of observation. We have therefore normalized variability amplitudes to a time-scale of 1 week, assuming the power spectrum slope seen in local AGN ($\alpha = 1.5$). This is also used to correct for time dilation effects since the frequency of variations from distant quasars will be decreased, lowering the measured amplitude of variability for observations of finite length.

A further correction is made for the effects of irregular binning. Low signal-to-noise light curves tend to have longer time bins for which high frequency variations are smeared out. The details of the correction methods used can be found in Almaini et al (2000).

5 THE RESULTS

The maximum likelihood estimates for the corrected intrinsic variability amplitudes of all 156 quasars are displayed in Fig. 2 and 3. The size of the points in Fig. 2(a) and 3(a) indicate relative flux. This is done in order to distinguish objects of higher signal-to-noise. Nearly half the sample (69 QSOs) give a non-zero maximum likelihood estimate of variability amplitude. The remaining QSOs can only provide upper limits, mainly due to low signal-to-noise.

Figure 4. Variability amplitude as a function of luminosity over 3 redshift ranges. The line plotted is the best fit relation to local ($z < 0.1$) AGN found by Nandra et al (1997).



Treating the entire sample as one ensemble, the corrected mean ensemble variability is: $\sigma = 0.15 \pm 0.01$ ($\sigma = 0.16 \pm 0.01$ uncorrected) on a time-scale of 1 week.

5.1 Correlations With Redshift And Luminosity

In Fig. 2 and 3 we display the variability amplitude as a function of luminosity and redshift. The data are split into 6 luminosity bins each of ~ 0.5 dex, and 11 redshift bins each of $\delta z = 0.3$. The ensemble variability amplitudes were calculated for each bin by combining the individual light curves and performing a maximum likelihood analysis as described in section 4.

Immediately apparent in Fig. 2(b) is an anti-correlation between quasar luminosity and variability amplitude. A power law fit to the individual quasars gives the best fit relation: $\sigma \propto L_X^{-\beta}$ where $\beta = 0.18 \pm 0.05$ (plotted as a dot-dash line). This gives a fairly poor fit to the ensemble points, mainly due to some highly variable, high luminosity QSOs. However, a power law fit to QSOs with redshift less than 2 (solid line, $\beta = 0.27 \pm 0.05$) passes through the majority of the ensemble points and is very close to the average relation found for local AGN (plotted as a dashed line). The errors quoted here are 68 per cent confidence limits for the slope on allowing the normalization to float to its optimum value.

For the redshift dependence (Fig. 3b), it is reasonable to expect a certain amount of degeneracy with luminosity. This effect appears to dominate at low and medium redshifts. At redshifts beyond ~ 2 , an upturn in variability is observed which cannot be explained as a consequence of the known trend with luminosity.

In order to decouple the effects of luminosity and redshift, the variability amplitude was plotted as a function of luminosity for

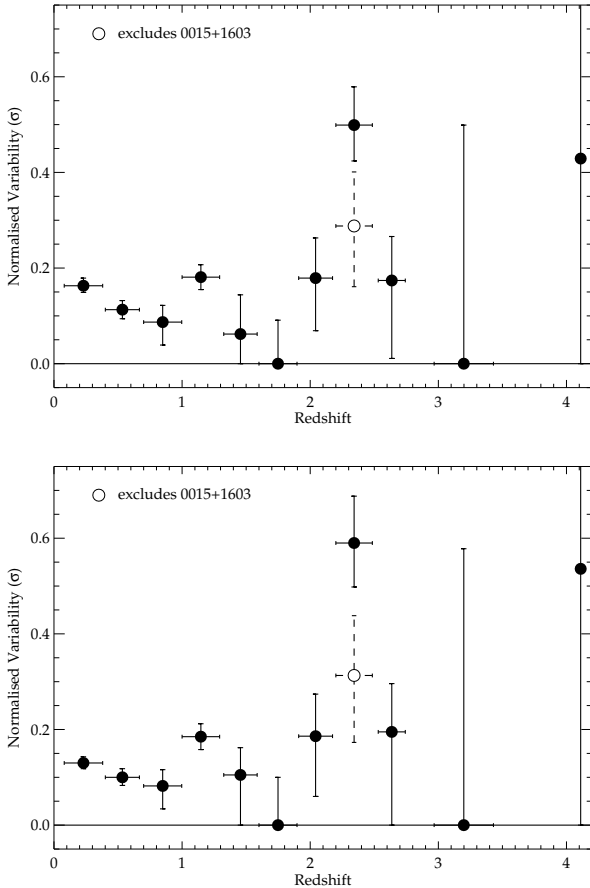
Table 2. Showing agreement between redshift ensembles from Fig. 4, and the best fit relation to local AGN found by Nandra et al ($\sigma \propto L_X^{-0.355}$)

QSO sample	$\chi^2_{\text{red}}^2$ fit to local AGN	Probability
$z < 1$	0.1	87%
$1 < z < 2$	1.7	17%
$z > 2$	12.9	0.00001%
$z > 2$ (excl. 0015+1603)	2.0	14%

3 redshift intervals (Fig. 4). The luminosity bins for each redshift interval overlap, providing a measure of the change in variability amplitude as a function of redshift. Comparing the first 2 redshift intervals we find no significant difference in the $\sigma - L_X$ relation. The anti-correlation between variability and luminosity appears to be unchanged out to a redshift of 2. To compare this with the relationship for local AGN, the power-law slope found by N97 is plotted on Fig. 4. This has been normalized to fit the points in the first redshift interval.* The reduced χ^2 values given in Table 2 compare the points in each redshift range with the normalized local AGN relation. Low values for the first 2 intervals display the observed

* It would be incorrect to use the normalization of N97, mainly due to the different observation lengths used (typically less than one day) and the different spectral range used to calculate luminosities. Crude corrections based on a standard power spectrum and X-ray spectral index give variability amplitudes around a factor of 2 lower for the N97 AGN. Given the uncertainties in these corrections and the differing methods of calculating variability amplitudes, this is not thought to be significant.

Figure 5. Variability amplitude as a function of redshift after removing the luminosity dependence (normalizing to $L_X = 10^{45}$). In (a) we use the best-fit power law to QSOs of $z < 2$ of $L_X^{-0.27}$. In (b) the relation for local AGN from Nandra et al (1997) of $L_X^{-0.355}$ is used.



close agreement with local AGN. The high value of reduced χ^2 for $z > 2$ can be mostly attributed to the object 0015+1603. However, once this object is removed, the hypothesis that these quasars follow the local $\sigma - L_X$ relation can still be rejected at the 85 per cent confidence level. Considering that all 3 points also show an ‘excess’ variability indicates that high redshift QSOs may not be well characterized by the variability-luminosity correlation of local AGN.

The upturn in variability seen for the highest redshift quasars in our sample can be quantified by fitting the N97 slope to the ensemble points in the redshift interval $z > 2$. This can then be compared to the fit for the $z < 1$ redshift interval. We find, at a fixed luminosity, that high- z QSOs are more variable than low- z QSOs by $\delta\sigma = 0.11$. An alternative interpretation is that at a fixed variability, high- z QSOs are more luminous by a factor of 16. If we exclude the variable quasar 0015+1603 (see section 6), the best fit requires $\delta\sigma = 0.06$ or an increase in luminosity by a factor of 6.

5.2 Characterizing the redshift dependence

In order to illustrate the redshift dependence of QSO X-ray variability, we attempted to remove the effect of the luminosity dependence by normalizing values to a luminosity of $L_X = 10^{45}$ ergs s^{-1} . Due to the close agreement between the first 2 redshift inter-

vals observed in Fig. 4, this was first done using the best fit power-law to QSOs with $z < 2$ ($\sigma \propto L_X^{-0.27}$). The results are plotted in Fig. 5. The low redshift ensembles (below $z \sim 2$) in Fig. 5(a) still appear to display a downward trend. A minimum is observed at a redshift of ~ 1.7 where the level of variability becomes consistent with zero. In contrast, the high redshift ensembles ($z > 2$) display an increase in variability. In Fig. 5(b) we use the luminosity relation found for local AGN (N97) to normalize variability amplitudes. Here the redshift ensembles for QSOs of $z < 1$ are noticeably flatter. Evidence for the minimum observed in Fig. 5(a) has become less significant. However, beyond $z \sim 2$, the increase in variability is more pronounced.

6 PROPERTIES OF HIGH-Z VARIABLE QSOs

The apparent increase in variability seen in high redshift QSOs may be due to the inclusion of a new population of objects rather than differences in the ‘typical’ population. Narrow-line Seyfert 1s are known to exhibit enhanced variability (Boller et al 1996, Leighly 1999) and could be responsible for this upturn if their high- z equivalents were more prevalent than they are today. In order to test this hypothesis, the identifications for the 12 QSOs that exhibit detected variability at redshifts greater than 1.9 (i.e. the last 5 redshift intervals in Fig. 3(b) & 5), were studied in more detail (Fig. 6 and Table 3). All the QSOs with adequate optical spectra were found to contain broad permitted lines (> 3000 km s^{-1} FWHM). In one object, 0015+1603, the optical grism spectrum was not of sufficient quality to determine linewidths. This object also displays a steep X-ray spectrum, so is a (potential) NLS1 candidate. 0015+1603 was the highest luminosity object in the sample with a high significance detection of variability. To determine the effect of this steep-spectrum QSO on the characteristics of the sample, the variability analysis was repeated with the object removed. The affected bins are plotted as unfilled points in Fig. 1 - 4. Removing this highly variable object decreases the significance of the upturn in variability for the high- z sample, but does not affect the direction of the trend.

7 IMPLICATIONS FOR QUASAR MODELS

7.1 The $\sigma - L_X$ anti-correlation

The relation between X-ray variability and luminosity, reliably identified for local AGN, is here seen to continue to redshifts of ~ 2 . However, there is still no definitive explanation for the anti-correlation. In particular, it is unclear whether variability is intrinsically linked with luminosity, or whether the link is to a third parameter that happens to scale with luminosity. If the upturn in variability observed at high redshifts is real, then an extra parameter must exist.

A change in measured variability amplitude can occur when the power spectrum of a quasar light curve is shifted in either amplitude or time-scale. At present these cannot be distinguished as features in the power spectrum (such as a turn-over of the power law at low frequency) have only been identified for the most well studied AGN (e.g. Edelson & Nandra 1999, Pounds et al 2001). This leaves us with a variety of possible explanations for the $\sigma - L_X$ relation, for example:

- A flaring accretion disk may cause the observed correlation in two ways. The luminosity may be related to i) the *number* of flares present on the disk (assumed to be all identical), or ii) the *size* of

Table 3. Notes on high- z variable quasars.

Name X-ray source name	RA, Dec. (J2000.0)	z	$\log L_X$ (0.1-2.4keV)	Variability (σ)	Notes
1118+1354 RX J112106.0+133825	11 21 06.00, +13 38 25.1	1.94	45.55	0.15 +0.52, -0.15	ROSAT spectrum gives $\alpha \sim 0.3$, Ly α , CIV present Faint emission line quasar (Weedman 1985)
[HBC98] 031 RX J105331.8+572454	10 53 31.80, +57 24 53.8	1.956	45.74	0.13 +0.07, -0.09	Broad SiIV, CIV, CIII] (Lehmann et al 2000)
0438-1638 1E 0438-166	04 40 26.478, -16 32 34.60	1.96	45.49	0.45 +0.39, -0.29	Broad Ly α , CIV (Osmer, Porter & Green 1994)
MS 0104.2+3153 2RXP J010659.1+320920	01 06 58.756, +32 09 18.01	2.027	46.01	0.40 +0.18, -0.15	Broad CIV, SiIV (Gioia et al 1986), BAL quasar with component from foreground IGM (Komossa & Bohringer 1999)
SGP3X:021 SGP 3:48	00 54 47.29 -28 31 54.8	2.097	45.30	0.46 +0.56, -0.46	Broad Ly α , CIV (> 3000 km/s, Boyle et al 1990)
0015+1603 2RXP J001749.5+161948	00 17 45.05, +16 19 52.6	2.20	46.51	0.31 +0.08, -0.06	Steep ROSAT spectrum ($\alpha \sim 2.8$) Ly α , CIV present (Anderson & Margon 1987)
F864X:013 (unpublished)	13 43 09.2, -00 22 57	2.21	45.27	0.51 +0.43, -0.31	Broad CIII, CIV (> 3000 km/s, Almaini 1996)
F864X:086 RX J1343.4+0001	13 43 29.20, +00 01 33.0	2.347	45.51	0.44 +0.21, -0.15	ROSAT spectrum: $\alpha = 0.6$, Narrow Ly α , CIV (Almaini et al 1995) Broad H α , no H β , type 1.9 QSO (Georgantopoulos et al 1999)
CRSS J1415.1+1140 2RXP J141511.7+114000	14 15 11.20 +11 40 03.0	2.353	45.48	0.97 +0.72, -0.58	Broad Ly α , CIV (Boyle et al 1997)
POX 042 2RXP J120044.8-185952	12 00 44.975, -18 59 45.04	2.453	46.04	0.15 +0.21, -0.15	Broad CIV, SiIV,OIV] (Ulrich 1989)
0315-5522 [ZMH99] X036-04	03 16 50.40, -55 11 09.9	2.531	45.81	0.15 +0.10, -0.11	Broad Ly α , CIV, Si+OIV] (Zamorani et al 1999)
Q0000-26 2RXP J000322.6-260312	00 03 22.909, -26 03 16.83	4.111	46.08	0.22 +0.36, -0.22	Broad Ly α , CIV, SiIV (Schneider et al 1989)

the individual flares. In the first case, an increase in the number of overlapping flares would act to ‘smear out’ the observed variability leading to an amplitude shift in the quasar power spectrum. The second case could lead to a time-scale effect if flares of longer duration are responsible for the increased luminosity.

- X-ray variability time-scale may directly scale with black hole mass if, for example, the emission occurs at a fixed number of Schwarzschild radii.

- Regardless of black hole mass, variability may depend on X-ray source size, which could in turn depend on luminosity.

Recent studies by Ptak et al (1998) show that most low-luminosity AGN (LLAGN) display very little X-ray variability, in marked contrast to the relation found by N97. However, these objects are expected to harbour relatively massive black holes with low accretion rates. Iwasawa et al (2000) studied the variability of a dwarf Seyfert (NGC 4395) which is thought to contain a small black hole ($\sim 10^5 M_\odot$). They find a large variability amplitude consistent with an extrapolation of the power-law fit to the $\sigma - L_X$ relation for the sample of N97. This would suggest that X-ray variability correlates with black hole mass, rather than directly with luminosity.

7.2 Explaining the high-redshift upturn

Given the possible reasons for the $\sigma - L_X$ anti-correlation, we can now identify potential causes for a high-redshift upturn in variability. It is tempting to think this may be simply due to a smaller typical black hole mass at these early epochs. In practice, this scenario does not work. Smaller black holes may lead to increased variability, but they should also lead to lower luminosities. These QSOs would then just fit an extrapolation of the measured $\sigma - L_X$ relation. Therefore, we may be seeing an intrinsic change in the behaviour of these objects. For the same variability seen in local AGN, these high redshift quasars appear almost an order of magnitude more luminous. The root of this shift in behaviour could be a change in the following parameters:

Intrinsic change in luminosity (i.e. accretion efficiency).

It seems reasonable to assume the amplitude of variability is linked with a global property of the QSO, such as black hole mass. The luminosity of the quasar must in some way be related to the rate of fueling (\dot{M}). Seeing a different $\sigma - L_X$ relation at high redshift then suggests that for a given black hole mass, the high- z quasars must have a greater rate of fueling, in other words, they are accreting at a higher fraction of the Eddington limit. Is it then feasible that $z > 2$ QSOs are accreting more efficiently than local AGN by almost an order of magnitude?

The Eddington ratio for local AGN has been relatively well con-

Figure 6. High-z variable QSOs.

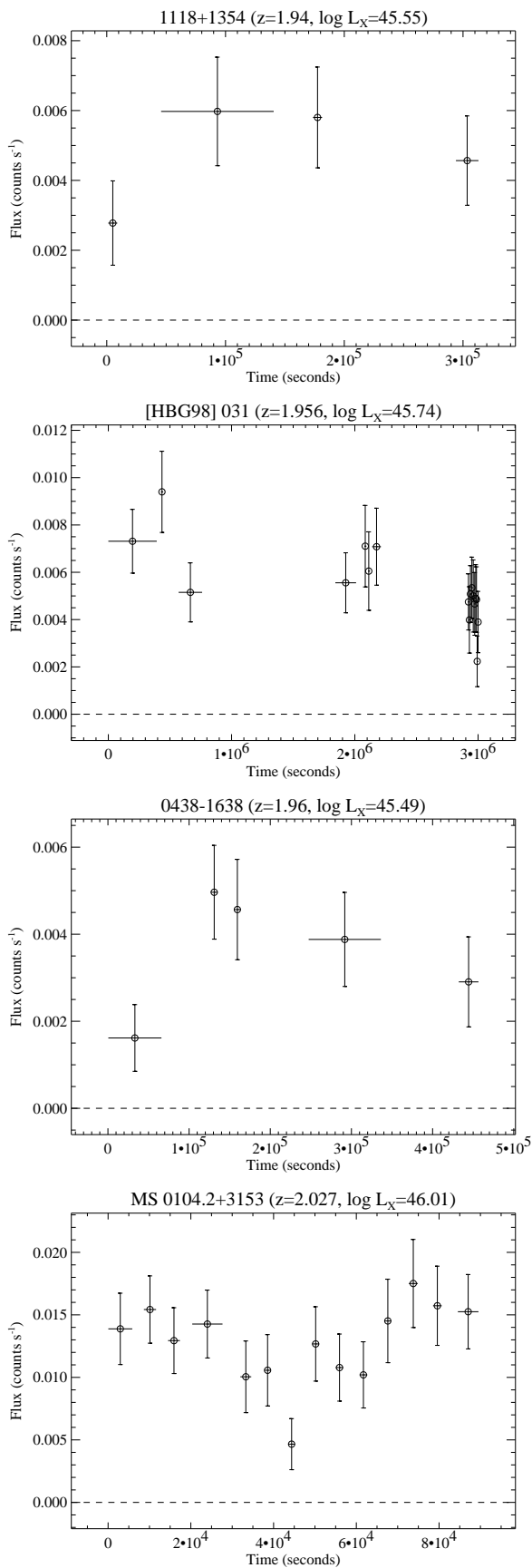


Figure 6. High-z variable QSOs.

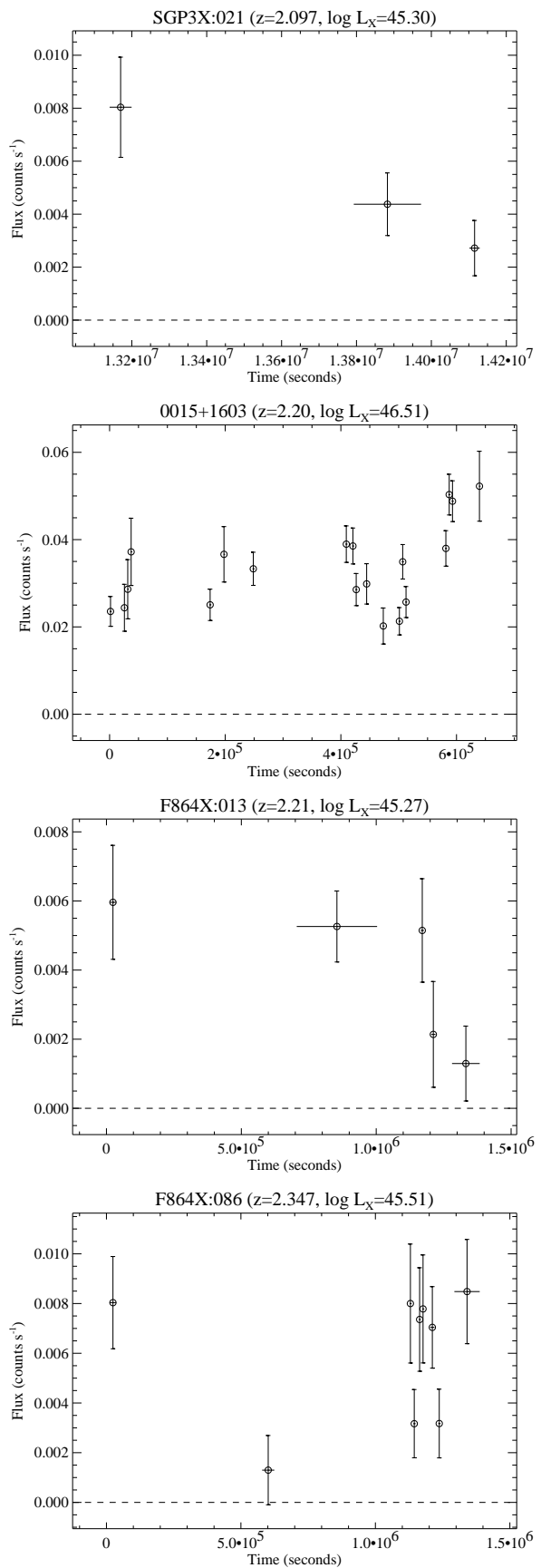
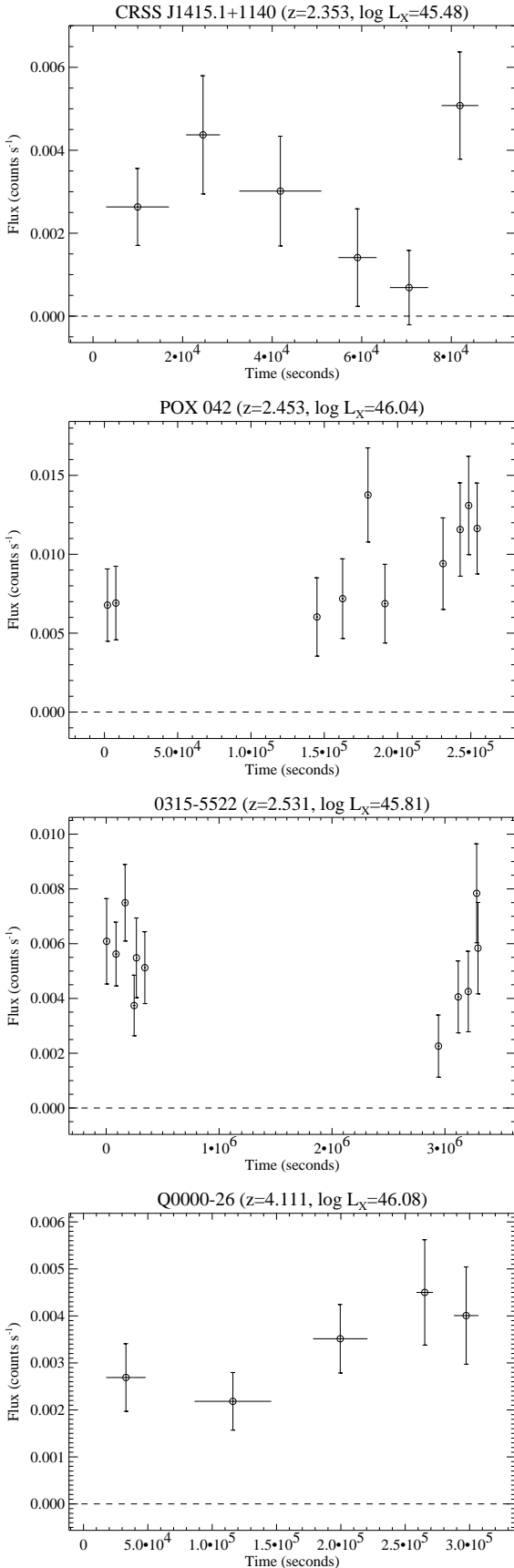


Figure 6. High- z variable QSOs.

strained. Wandel et al (1999), use reverberation methods to accurately define the Eddington ratio for local Seyferts. They find $L/L_{Edd} \approx 0.01 - 0.3$, though there is a strong trend of the Eddington ratio to increase with luminosity. The necessary increase in accretion efficiency, to allow a typical high redshift QSO to be almost an order of magnitude more luminous, would imply these objects were accreting very close to the Eddington limit.

If this increase in accretion efficiency is real, the cause must lie with the environmental conditions at these redshifts. It is plausible that early QSOs enjoyed a more fuel-rich environment.

Intrinsic change in variability. The upturn may also be characterized as an increase in variability for QSOs of the same luminosity. Possible scenarios include:

- (i) The X-ray emitting region is physically smaller in size, but of greater intensity, for high- z QSOs. This could occur if the emission region was located at a smaller number of Schwarzschild radii.
- (ii) In the flaring accretion disk model, there may be a smaller number of more luminous flares for high- z QSOs. Enhanced magnetic fields could conceivably provide a mechanism to achieve this.
- (iii) It is possible that some short time-scale variability is caused by temporary obscuration of the X-ray source. This could be due to broad-line clouds moving across the line of site, or perhaps rotations of a warped accretion disk. It is feasible that high- z QSOs may contain more of this obscuring material, leading to enhanced variability over these time-scales.

Spectral sampling. The ROSAT band of 0.1 - 2.4 keV used for the variability analysis, will sample higher rest frame energies as redshift increases. For a QSO at a redshift of 2.5, variability will actually be measured in the rest frame band of 0.35 - 8.4 keV. The increased variability observed at high redshift could therefore be due to intrinsic spectral variability. This would require QSOs to be more variable at harder energies indicating a different source for these X-rays. However, N97 showed there was a strong correlation between hard band (2-10keV) and soft band (0.5-2 keV) variability in local AGN. Where the correlation breaks down they find greater variability in the soft band.

Emergence of a new population. An increase in mean AGN variability would be observed if a subset of highly variable AGN (such as Narrow-line Seyfert 1s) were more prevalent at high redshift. Based on the optical spectra however, we find no evidence that this is due to the emergence of a ‘narrow-line’ population (see section 6).

Given the low signal-to-noise of this data it is difficult to constrain these models beyond the general descriptions given here. A full power spectrum analysis is required to fully characterize and confirm this trend. This may be possible with long observations using XMM-Newton, XEUS or Constellation-X.

8 CONCLUSIONS

We have measured the amplitude of short-term X-ray variability of 156 radio quiet quasars taken from the ROSAT PSPC archive over a redshift range of 0.08 - 4.11. In order to identify trends with luminosity and redshift we have combined light curves into ensembles. For QSOs out to redshift ~ 2 we find the amplitude of variability decreases with luminosity as $\sigma \propto L_X(0.1 - 2.4 \text{ keV})^{-\beta}$ with $\beta = 0.27 \pm 0.05$. This is comparable to the relation found for local AGN. The behaviour of QSO variability amplitude with redshift is

approximately flat out to $z \sim 2$, although there is some suggestion of a minimum at $z \sim 1.7$. Beyond redshift ~ 2 there is some evidence for an increase in QSO X-ray variability. The hypothesis that these quasars observe the local $\sigma - L_X$ relation found by Nandra et al (1997), is marginally rejected. We explore the possible reasons for this upturn. If the amplitude of X-ray variability is linked to black hole mass, this would imply nearly an order of magnitude increase in accretion efficiency for typical high-redshift QSOs.

The data used to produce any of the figures in this paper may be obtained by emailing James Manners at jcm@roe.ac.uk.

ACKNOWLEDGMENTS

This research has made use of data obtained from the Leicester Database and Archive Service at the Department of Physics and Astronomy, Leicester University, UK. James Manners acknowledges the support of a PPARC Studentship.

REFERENCES

- Almaini O., Boyle B.J., Griffiths R.E., Shanks T., Stewart G.C. & Georgantopoulos I., 1995, MNRAS, 277, L31
- Almaini O., 1996, Ph.D. thesis, Durham Univ.
- Almaini O., Lawrence A., Shanks T., Edge A., Boyle B.J., Georgantopoulos I., Gunn K.F., Stewart G.C., Griffiths R.E., 2000, MNRAS, 315, 325
- Anderson S.F. & Margon B., 1987, ApJ, 314, 111
- Boller T., Brandt W.N., Fink H., 1996, A&A, 305, 53
- Boyle B.J., Fong R., Shanks T., Peterson B.A., 1990, MNRAS, 243, 1
- Boyle B.J., Wilkes B.J. & Elvis M., 1997, MNRAS, 285, 511
- Edelson R., Nandra K., 1999, ApJ, 514, 682
- Georgantopoulos I., Almaini O., Shanks T., Stewart G.C., Griffiths R.E., Boyle B.J., Gunn K.F., 1999, MNRAS, 305, 125
- Gioia I.M., Maccacaro T., Schild R.E., Giommi P., Stocke J.T., 1986, ApJ, 307, 497
- Green A.R., McHardy I.M. & Lehto H.J. 1993, MNRAS 265, 664
- Hasinger G., Burg R., Giacconi R., Schmidt M., Trumper J., Zamorani G., 1998, A&A, 329, 482
- Iwasawa K., Fabian A.C., Brandt W.N., Kunieda H., Misaki K., Reynolds C.S. & Terashima Y., 1998, MNRAS, 295, L20
- Iwasawa K., Fabian A.C., Almaini O., Lira P., Lawrence A., Hayashida K. & Inoue H., 2000, MNRAS, 318, 879
- Komossa S. & Bohringer H., 1999, A&A, 344, 755
- Lawrence A. & Papadakis I. 1993, ApJ 414, L85
- Lehmann I., Hasinger G., Schmidt M., Gunn J., Schneider D., Giacconi R., McCaughrean M., Trumper J., Zamorani G., 2000, A&A, 354, 35
- Leighly K.M., 1999, ApJS, 125, 297
- McHardy I. et al., 1998, MNRAS, 295, 641
- Nandra K., George I.M., Mushotzky R.F., Turner T.J., Yaqoob T., 1997, ApJ, 476, 70
- Osmer P.S., Porter A.C. & Green R.F., 1994, ApJ, 436, 678
- Papadakis I.E. & Lawrence A., 1993, Nat, 361, 250
- Papadakis I.E. & Lawrence A., 1995, MNRAS, 272, 161
- Pounds K., Edelson R., Markowitz A., Vaughan S., 2001, ApJ, 550, L15
- Ptak A., Yaqoob T., Mushotzky R., Serlemitsos P., Griffiths R., 1998, ApJ, 501, L37
- Schmidt M., Hasinger G., Gunn J., Schneider D., Burg R., Giacconi R., Lehmann I., MacKenty J., Trumper J., Zamorani G., 1998, A&A, 329, 495
- Schneider D.P., Schmidt M., Gunn J.E., 1989, AJ, 98, 1507
- Shanks T., Georgantopoulos I., Stewart G.C., Pounds K.A., Boyle B.J. & Griffiths R.E., 1991, Nat, 353, 315
- Turner T.J., 1988, Ph.D. thesis, Leicester Univ.
- Ulrich M.H., 1989, A&A, 220, 71

- Veron-Cetty M.-P., Veron P., 1993, ESO Scientific Report No. 13
- Veron-Cetty M.-P., Veron P., 2000, ESO Scientific Report No. 19
- Wandel A., Peterson B.M., & Malkan M.A., 1999, ApJ, 526, 579
- Weedman D.W., 1985, ApJS, 57, 523
- Zamorani G., Mignoli M., Hasinger G., Burg R., Giacconi R., Schmidt M., Trumper J., Ciliegi P., Gruppioni C., Marano B., 1999, A&A, 346, 731